Iterative Spatial Demapping for Two Correlated Sources with Power Control over Fading MAC

Khoirul Anwar* and Tad Matsumoto*,**

*School of Information Science, Japan Advanced Institute of Science and Technology (JAIST)
Asahidai 1-1, Nomi, Ishikawa, Japan 923–1211,
E-mail: {anwar-k, matumoto}@jaist.ac.jp
**Centre for Wireless Communications (CWC), University of Oulu, Finland, FI-90014
E-mail:tadashi.matsumoto@ee.oulu.fi

Abstract—This paper proposes a simple coding structure with iterative spatial demapper (ISM) for single carrier transmission of two correlated sources (with *instantaneous power control*) over fading multiple access channel (Fading MAC) where the receiver has only a single receive antenna. The correlation between the sources is exploited via *vertical iteration* (*VI*) loop between the two decoders and analyzed based on the Slepian-Wolf (SW) coding theorem. The proposed structure, of which potential applications are sensor or relay systems requiring relatively small number of the transmission phases, can achieve turbo-like performance over Fading MAC even with short memory convolutional codes (CC). The rate-1 doped accumulator (D-ACC) is used to flexibly adapt the variation of the correlation between the sources which makes the convergence tunnel between the demapper and decoder open until a point very close to (1,1) mutual information (MI) point. The results of computer simulations confirm that the proposed structure can achieve close performance to the Slepian-Wolf/Shannon limit of two correlated sources using single transmission phase.

I. INTRODUCTION

In multi-node communications, the correlation in information between the multiple sources can be utilized to reduce the energy consumption [1] for reliable data transmission from multiple sources to a common receiver. A goal of this paper is to propose a technique that can make efficient use of the source correlation in the framework of multiple access channel (MAC) with single antenna receiver.

Despite the volume of publications describing transmission techniques for *independent* multiple sources, to the authors' best knowledge, only a few simple techniques for application of *correlated* sources in wireless sensor or relaying systems have been investigated from the viewpoint of Slepian-Wolf (SW) coding system.

The SW coding theorem, introduced by Slepian and Wolf in 1973 [2], has drawn much attention recently with the aim of its applications to variety of systems such as sensor networks [3], and recently to relay and cooperative network systems [4].

The SW coding theorem specifies achievable rate regions of multiple sources, $\mathcal{R}_1$ and $\mathcal{R}_2$, when considering the lossless compression of two correlated sources b_1 and b_2 sending data
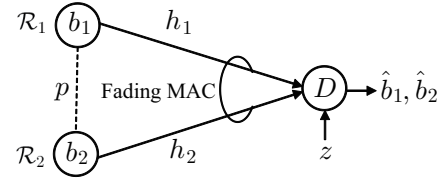
Fig. 1. Transmission of two correlated sources with joint entropy $\mathcal{H}(b_1, b_2) = 1 + \mathcal{H}(p)$ over fading multiple access channel (Fading MAC) to a common destination D

to a common joint decoder as shown by Fig. 1. The region is an unbounded polygon with two corner points, where b_1 is compressed at its entropy $\mathcal{H}(b_1)$ while b_2 can be compressed at a smaller rate than its entropy $\mathcal{H}(b_2)$, but larger than their conditional entropy $\mathcal{H}(b_2|b_1)$ or vice versa. The SW bound is given by the three inequalities,

$$\mathcal{R}_1 \geq \mathcal{H}(b_1|b_2), \qquad (1)$$
$$\mathcal{R}_2 \geq \mathcal{H}(b_2|b_1), \qquad (2)$$
$$\text{and} \quad \mathcal{R}_1 + \mathcal{R}_2 \geq \mathcal{H}(b_1, b_2), \qquad (3)$$

where $\mathcal{H}(b_1, b_2)$ is the joint entropy. The contribution of SW coding theorem is the discovery that the compression can be performed even if both sources are encoded separately as long as the joint decoder is able to *know* or *estimate* the source correlation.

In this paper, we propose for single carrier signaling a simple structure of SW coding systems using single transmission phase and single antenna receiver for two correlated sources using iterative spatial demapper (ISM), denoted as SW-ISM structure, for fading multiple access channel (Fading MAC) with *instantaneous power control*.[1] The receiver performs ISM demapper combined with iterative decoding separated by interleavers, where the correlation between the two sources is exploited using a *vertical iteration* (*VI*) loop; the detection of sources b_1 and b_2 are performed by *horizontal iteration* (*HI*) loop.

[1]The analysis and results on general Fading MAC (without instantaneous power control) are not presented in this paper due to the space limitation. However, the results presented in this paper is also valid for general Fading MAC.

Spatial mapping is presented, for example, in [5] for multiple-input multiple-output (MIMO) systems, where the optimal spatial mapping for BPSK can outperform the conventional, called 'serial-to-parallel (S/P)', mapping. However, the mapping optimization is difficult for independent transmission of separate sources,[2] (or other non-MIMO systems) which *by nature* results in Gray mapping that has no benefit for iterative processing even *a priori* information is available.

To solve the problem, inspired by [6], this paper proposes iterative spatial demapper combined with the rate-1 doped accumulator (D-ACC); D-ACC improves the demapper performance even with Gray mapping by "bending up" the right hand side of the its extrinsic information transfer (EXIT) curve [7]. Furthermore, it results in a better matching to the decoder of convolutional code's EXIT curve to achieve performance very close to the SW/Shannon theoretical limit. To the best of our knowledge, this paper for the first time proposes MAC/Slepian-Wolf results (single transmission phase), therefore the performances are presented with physical layer network coding (PLNC) [8] as the baseline comparison.

This paper is organized as follows: In Section II, we describe the system model assumed in this paper. In Section III, we provide detailed descriptions of our proposed the SW-ISM structure, which is followed by EXIT chart analysis in Section IV to provide in-depth consideration on the joint decoding of the correlated sources. We also provide briefly the results of theoretical analysis of the SW capacity region over Fading MAC and its performance evaluation in Section V. Finally, we conclude this paper in Section VI with some concluding remarks.

II. SYSTEM MODEL

In this paper, we consider single carrier signaling.[3] Fig. 1 shows a block-diagram of the system we consider, where the binary streams b_1 and b_2 are encoded separately, and the sources do not communicate each other. Puncturing for each coded source may be performed to adjust the rates $\mathcal{R}_1$ and $\mathcal{R}_2$ including compression and channel coding.

The encoded sources b_1 and b_2 are then mapped on to symbols s_1 and s_2 with $\mathbb{E}\{s_1\} = 1$, $\mathbb{E}\{s_2\} = 1$, respectively, using binary-phase shift keying (BPSK).[4] The symbols s_1 and s_2 are transmitted simultaneously with powers P_1 and P_2, respectively, such that transmission of both sources requires only *one* transmission phase.

Block wise transmission is assumed. The channels between transmit antenna 1 and 2 to the single receive antenna are both assumed to be one-path (block) Rayleigh distributed fading channel with instantaneous power control so that the complex channel coefficient for source 1 and 2 are $|h_1| = 1$ and $|h_2| = 1$, respectively.[5]

[2]The encoder and modulator do not communicate each other.

[3]An extension to other signaling schemes, such as multicarrier systems as well as their mixture systems, is rather straightforward.

[4]There is no restriction to other higher order modulations.

[5]An extension to multipath Rayleigh fading channel is possible by turbo equalization, e.g., frequency domain soft-cancellation minimum mean square error (FD/SC-MMSE) as in [9], [10].
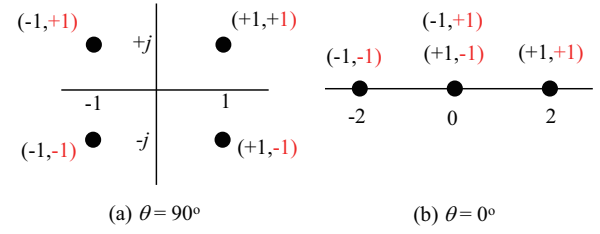

Fig. 2. Constellations of spatially separated two BPSK symbols with channel phase difference θ of (a). $90°$ and (b). $0°$

TABLE I
SUMMARY OF MAC MODEL DEFINITIONS

$|h_1|, |h_2|$	$\theta = \angle(h_1, h_2)$	Noise	MAC
1	$0°$	$N = 0$	Binary Erasure MAC
1	$0°$	$N > 0$	Gaussian MAC [11]
1	random	$N > 0$	Fading MAC (Power Control)
Rayleigh	random	$N > 0$	Fading MAC

Due to the simultaneous transmission from two transmit antennas to a single receive antenna at the receiver, the received signal r is a superposition of the signals, as

$$r = h_1\sqrt{P_1}s_1 + h_2\sqrt{P_2}s_2 + z, \qquad (4)$$

where z is a noise component modeled by complex Gaussian random variable with zero mean and variance $\sigma_n^2/2$ per dimension, and hence the complex noise power is $N = \sigma_n^2$. The channel state information (CSI) is assumed to be known to the receiver, however, since we consider an instantaneous power control, the magnitude of CSI is known (but the phase difference $\theta = \angle(h_1, h_2)$ is not known) to the transmitter. Hence, the received signal-to-noise power ratio (SNR) for source 1 and 2, respectively, are defined as

$$\gamma_1 = \frac{|h_1|^2 P_1}{N} = \frac{P_1}{N}, \quad \text{and} \quad \gamma_2 = \frac{|h_2|^2 P_2}{N} = \frac{P_2}{N}. \qquad (5)$$

The effect of superposition depends on the complex channel gains h_1 and h_2 and their random variable phase difference θ. With $\theta = 90°$ the constellation point of the received symbols is plotted in Fig. 2(a)[6] with $j = \sqrt{-1}$, while with $\theta = 0°$ is shown in Fig. 2(b), both for $P_1 = P_2 = 1$. In this paper, we use terminology *Fading MAC* with instantaneous power control since $\theta = random$ and the *power is controlled* such that $|h_1| = |h_2| = 1$. The other MAC models for different parameter settings are summarized in Table I.

III. PROPOSED SLEPIAN-WOLF ITERATIVE SPATIAL DEMAPPING (SW-ISM) STRUCTURE

Based on insightful findings in [9], [10] and [12], we propose SW-ISM structure that use only one transmission phase, of which the receiver has a common iterative spatial demapper and two short memory convolutional decoders. The proposed SW-ISM structure is shown in Fig. 3.

[6]Normalization by $\sqrt{2}$ is not needed because it is a composite symbol. Furthermore, the results of superposition with $\theta = 90°$ are not $\{+1, -1, +j, -j\}$.

A. Correlated Sources Model

A simple bit flipping model [13] is used to parameterize the correlation between the sources $b_1 = [b_1^1, b_1^2, \cdots, b_1^k, \cdots]$ and $b_2 = [b_2^1, b_2^2, \cdots, b_2^k, \cdots]$. We assume that the sequence b_1 satisfies the i.i.d condition with $\Pr(b_1^k = 0) = 0.5$, $\Pr(b_1^k = 1) = 0.5$. Then, the sequence b_2 is defined as

$$b_2^k = b_1^k \oplus e^k, \tag{6}$$

where $\oplus$ indicates a modulo 2 addition and $e^k \in \{0, 1\}$ is the random variable for the k-th source bit with probabilities $\Pr(e^k = 1) = p$ and $\Pr(e^k = 0) = 1 - p$, which is independent of b_1^k. The conditional probability is then given by

$$\Pr(b_2^k = 0 | b_1^k = 1) = \Pr(b_2^k = 1 | b_1^k = 0) = p \tag{7}$$
$$\Pr(b_2^k = 0 | b_1^k = 0) = \Pr(b_2^k = 1 | b_1^k = 1) = 1 - p, \tag{8}$$

where parameter p can be in the range of $0 \leqslant p \leqslant 0.5$ [13].

With the source model described above, the sequences of the binary random variables b_1^k and b_2^k in source b_1 and b_2, respectively, are still i.i.d in terms of the bit index k (not temporarily correlated) and the appearances of 0 and 1 are equiprobable. Therefore, the corresponding entropy $\mathcal{H}(b_1) = \mathcal{H}(b_2) = 1$, while the conditional entropy of $\mathcal{H}(b_1|b_2)$, is given by

$$\mathcal{H}(b_1|b_2) = \lim_{k \to \infty} \frac{1}{k} H(b_2^1, \cdots, b_2^k | b_1^1, \cdots, b_1^k) = \mathcal{H}(p), \tag{9}$$

where $\mathcal{H}(p) = -p \log_2(p) - (1-p) \log_2(1-p)$ is a binary entropy of random sequence e. As a consequence, the achievable SW region $(\mathcal{R}_1, \mathcal{R}_2)$ with this model is given by

$$\mathcal{R}_1 \geq \mathcal{H}(p), \tag{10}$$
$$\mathcal{R}_2 \geq \mathcal{H}(p), \tag{11}$$
$$\text{and} \quad \mathcal{R}_1 + \mathcal{R}_2 \geq 1 + \mathcal{H}(p). \tag{12}$$

B. Transmitters

Two sources, b_1 and b_2, are transmitted from two separated antennas simultaneously. The bitstream b_1 is convolutionally encoded using C_1, interleaved by Π_1, doped accumulated, and modulated to form BPSK symbol s_1. The bitstream b_2 is first Π_0-interleaved, convolutionally encoded using C_2, interleaved by Π_2, doped accumulated and modulated to form BPSK symbol s_2.

The interleaver Π_0 is introduced to exploit the correlation knowledge via the *VI* loop at the receiver, while Π_1 and Π_2, which is longer than Π_0 is used to interleave the coded bits x and y to obtain sequences x' and y'.[7]

The rate-1 D-ACC [12] can be applied to fully exploit the correlation between the sources in SW systems. As shown in Fig. 3, D-ACC is performed after the interleaver. The structure of D-ACC is very simple since it is composed of a memory-1 systematic recursive convolutional codes (SRCC) with octal code generator of $([3, 2]3)_8$ followed by *heavy puncturing* of the coded bits so that overall *coding rate* $= 1$. With a doping

---

[7]A delay τ may be added to antenna 1 as a compensation of the delay because of interleaver Π_0 at source b_2.

---

rate Q, the D-ACC replaces every Q-th systematic bits with the accumulated coded bit.

At the receiver D-ACC decoding, denoted as D_{dacc}, is performed using Bahl-Cokce-Jelinek-Raviv (BCJR) algorithm [14] immediately after the demapper. It should be noted here that interleaver between D_{dacc} and the demapper is not needed because the extrinsic log-likelihood ratio (LLR) is not exchanged between them.

C. Receiver

The receiver consists of a common ISM demapper, two *HI* loops because two sources are considered, and *VI* loop to exploit the benefit of correlation between the sources. ISM demapper performs demapping of spatial constellation from r into s_1, symbol-by-symbol, with the help of *a priori* information for s_2, and vice versa, in the form of LLR provided by the decoder. The demapper output is extrinsic LLR which is fed into D_{dacc}, deinterleaved, and then decoded by D_1 or D_2.

Decoder D_1 and D_2 provide extrinsic LLR of the uncoded bits L_{e,D_1}^u and L_{e,D_2}^u, respectively, to performs *VI* loop to achieve additional coding gain by exploiting the correlation knowledge p. Decoders D_1 and D_2 also provide extrinsic LLRs of the coded bits L_{e,D_1}^c and L_{e,D_2}^c, respectively, for the *HI* loop to improve the ISM demapper performance by providing additional extrinsic LLRs.

1) ISM Demapper: As shown in Fig. 3, with the help of *a priori* information about s_1 provided by the decoder D_1 in the form of $L_{a_1,M}$, the demapper calculates the extrinsic LLR $L_{e_2,M}$ of the symbol s_2 from the received signal r by

$$
\begin{aligned}
L_{e_2,M} &= \ln \frac{\Pr(s_2 = +1|r)}{\Pr(s_2 = -1|r)} \\
&= \ln \frac{\sum_{\mathcal{S} \in \mathcal{S}_{+1}} \exp\left\{ -\frac{|r - h_1\sqrt{P_1}s_1 - h_2\sqrt{P_2}s_2|^2}{\sigma_n^2} + b_1 L_{a_1,M} \right\}}{\sum_{\mathcal{S} \in \mathcal{S}_{-1}} \exp\left\{ -\frac{|r - h_1\sqrt{P_1}s_1 - h_2\sqrt{P_2}s_2|^2}{\sigma_n^2} + b_1 L_{a_1,M} \right\}},
\end{aligned}
\tag{13}
$$

where $\mathcal{S}_{+1}$, $\mathcal{S}_{-1}$ are the sets of superposition symbols in (4) having symbol s_1 being $+1$ and -1, respectively, with $s_1 = 1 - 2b_1$. Similarly, with the help of *a priori* information about symbol s_2 provided by decoder D_2 in the form of $L_{a_2,M}$, the extrinsic LLR $L_{e_1,M}$ of symbol s_1 is calculated.

The extrinsic LLRs, $L_{e_1,M}$ and $L_{e_2,M}$ are then doped deaccumulated by D_{dacc}, deinterleaved by Π_1^{-1} and Π_2^{-1}, respectively, to provide *a priori* LLR, L_{a,D_1}^c and L_{a,D_2}^c, of the coded bits for the decoders D_1 and D_2.

2) Vertical Iterations and LLR Updates: Because the two sources are not fully correlated, i.e., $(p \neq 0)$, the extrinsic LLR of the uncoded information bits, obtained as a result of the BCJR algorithm, has to be *updated* to avoid error propagation via the *VI* loop. As in [13], we use the following probability
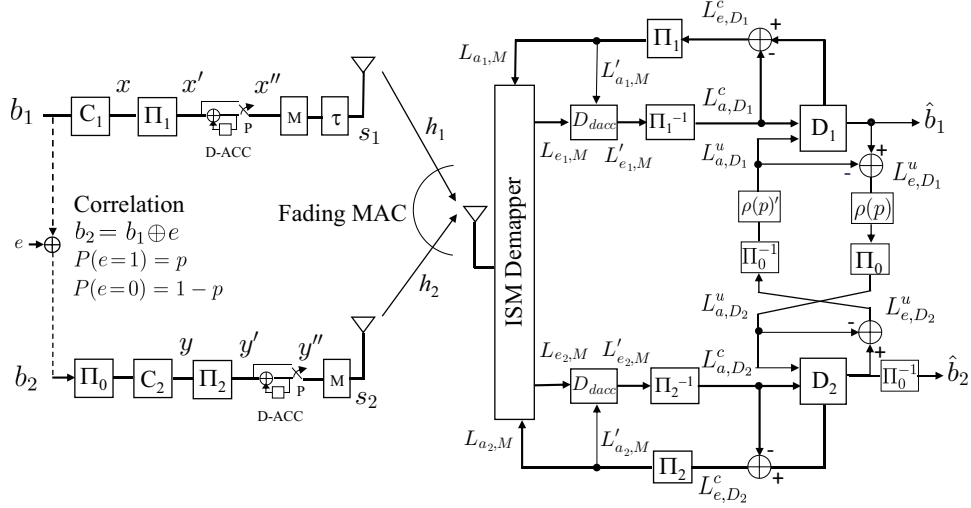
Fig. 3. The proposed single antenna receiver for two correlated sources with single transmission phase

update for b_2:

$$\Pr(b_2 = 0) = (1-p)\Pr(b_1 = 0) + p\Pr(b_1 = 1),$$
$$\Pr(b_2 = 1) = (1-p)\Pr(b_1 = 1) + p\Pr(b_1 = 0). \quad (14)$$

The probability update for b_1 is performed in the same way as (14). The LLR updating function $\rho(\cdot)$ corresponds to (14) for b_2 is

$$L^{b_2} = \rho(p, L^{b_1}) = \ln \frac{(1-p)e^{L^{b_1}} + p}{(1-p) + pe^{L^{b_1}}}, \quad (15)$$

where L^{b_1} and L^{b_2} are the extrinsic LLRs of b_1 and b_2, respectively. Similarly, the updating function for b_1, $L^{b_1} = \rho(p, L^{b_2})'$, is obtained from (15) by changing $L^{b_2}(L^{b_1})$ by $L^{b_1}(L^{b_2})$. In this paper, we assume that p is perfectly known to the receiver.[8]

IV. EXIT ANALYSIS

EXIT analysis is necessary to evaluate the convergence properties of the proposed iterative spatial demapper and its corresponding decoders with *VI* loops with the correlation p values as a parameter. We assume that $P_1 = P_2 = P$ so that the SNRs for source 1 and 2 are the same as $\gamma_1 = \gamma_2 = \gamma$. Because of the limited space, in this section we show only the EXIT chart with $\theta = 0°$, because of its most critical effect that results in the worst bit-error-rate (BER) performance. Fig. 4 shows for the source b_1 EXIT chart of the ISM demapper and the joint decoder (obtained via the *VI* loop) for $\gamma = \{-4.875, -2, 0\}$ dB with correlation values of $p = \{0.00, 0.10, 0.49\}$ with $\theta = 0°$.

The X-axis is mutual information (MI) between x'' and $L'_{a_1,M}$, denoted as $I_{a_1,M} = I(x''; L'_{a_1,M})$, and MI $I^c_{e,D_1} =$
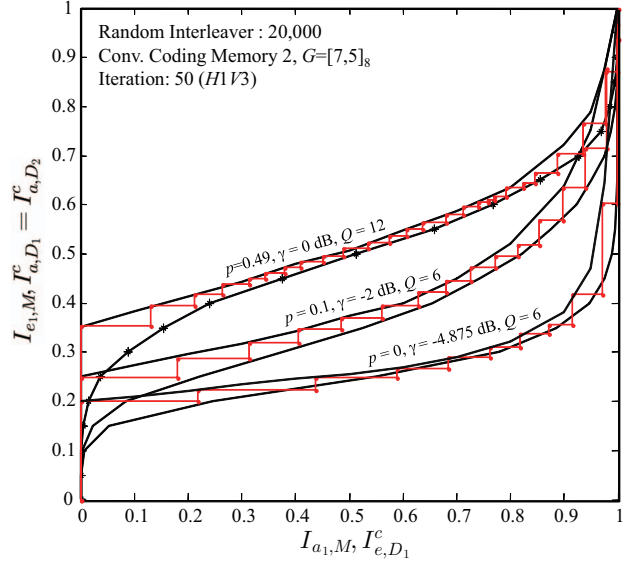

Fig. 4. EXIT chart of source b_1 at $p = \{0, 0.1, 0.49\}$

$I(x; L^c_{e,D_1})$, where x and x'' are shown in Fig. 3 and $L'_{a_1,M} = \Pi_1(L^c_{e,D_1})$ with $\Pi_1(\cdot)$ being the Π_1 interleaver function. Here,

$$L_{a_1,M}(k) \equiv \begin{cases} L'_{a_1,M}(k), & k \neq nP, n = 1, \cdots, K \\ 0, & \text{otherwise,} \end{cases} \quad (16)$$

where $L'_{a_1,M}(k)$ is the *a priori* LLR for D_{dacc} and k is the bit-index.

The Y-axis of Fig. 4 is MI $I_{e_1,M} = I(x''; L_{e_1,M}$ and $I^c_{a,D_1} = I(x; L^c_{e,D_1})$. It is important to note that by assuming that $I^c_{a,D_1} = I^c_{a,D_2}$ the decoder EXIT curve can be plotted in two dimensions (2D),[9] because the extrinsic LLRs $L_{e_1,M}$ and $L_{e_2,M}$ are produced by the same demapper. It should be

---

[8]When p is unknown to the receiver, it can be estimated using the technique in [13]. However, the estimation quality can be improved by the use of *a posteriori* LLR as shown in [10].

[9]Otherwise, the decoders' EXIT curve should be plotted in three dimensions (3D), since $I^c_{e,D_1} = T(I^c_{a,D_1}, I^c_{a,D_2})$ with $T(\cdot)$ being the decoders' EXIT curve transfer function.

noticed in Fig. 4 that the trajectory and EXIT curves of the ISM demapper and decoders are exactly consistent each other.

As observed from Fig. 4, the decay of ISM demapper EXIT curve depends on: (a) γ values, and (b) the doping rate Q. It is shown that small doping rate, $Q = 6$, is required when the correlation value p is small, while $Q = 12$ is needed when the correlation is closer to $p \approx 0.5$. The reason is that the bigger the p value the smaller the coding gain obtained by the LLR exchange via *VI* loops[10] and the help from the joint decoder diminishes. In this case, the ISM demapper should increase the doping rate Q such that the number of zero *a priori* LLR, $L_{a_1,M}(k) = 0$ in (16) decreases.

The EXIT curve of joint decoders depends on the correlation p, where the area under the decoder EXIT curve decreases equivalently to the SW coding rates η_{SW}. The detailed proportional relation between η_{SW} and the bit-flipping probability p is given by (18) as $\eta_{SW} \propto \{1 + \mathcal{H}(p)\}$. This relation is confirmed by the EXIT curves shown in Fig. 4. It is also observed from the figure that because of no intersection between the ISM demapper and decoder EXIT curves, turbo cliff happens at the corresponding threshold γs.

V. PERFORMANCE EVALUATION

A series of computer simulation was conducted to verify the effectiveness of the proposed SW-ISM structure for several values of bit-flipping probabilities p representing the correlation parameters. Binary sequence b_1 is generated randomly with length of 10,000 bits. The bits in b_1 was randomly flipped with probability of $p = \{0, 0.01, 0.1, 0.2, 0.3, 0.4, 0.49\}$, and randomly Π_0-interleaved to produce sequence b_2, as $b_2 = \Pi_0(b_1 \oplus e)$, where $\Pr(e = 1) = p$. Therefore, the length of interleaver Π_0 is also 10,000 bits.[11]

The binary sequences b_1 and b_2 are then independently encoded by the same memory-2 rate 1/2, $R_{c_1} = R_{c_2} = 1/2$, non-systematic non-recursive convolutional codes (NSNRCC) with a generator polynomial $G = [7, 5]_8$, resulting in two independent sequences x and y, each having length of 20,000 bits. The sequence x and y are further independently interleaved by random interleavers Π_1 and Π_2, respectively,[12] and then doped accumulated by D-ACC with doping rates $P = \{5, 6, 10, 12\}$.

BPSK symbols s_1 and s_2, $s_1 = 1 - 2b_1$ and $s_2 = 1 - 2b_2$, respectively, where the transmit power is set to $P_1 = P_2 = 1 = P$. The receiver is assumed to have perfect knowledge about the correlation p. We use activation ordering pattern $50(H1V3)$, which means that each one *HI* followed by 3 *VI* is repeated 50 times. The total iterations in maximum is, therefore, 2×50 *HI*s + 3×50 *VI*s for each block.

A. Theoretical Limit

The Slepian-Wolf and Shannon theorems states that the condition to achieve arbitrarily low BER for two correlated sources, b_1 and b_2, is given by (3).

---

[10]The *VI* loop disconnects D_1 and D_2 at an exact value of $p = 0.5$.

[11]This length is assumed to be enough to simulate the number of flipped bits e, especially for $p = 0.01$ since $0.01 \times 10,000 = 100$ bits are flipped.

[12]The length of interleavers Π_1 and Π_2 is, therefore, also 20,000 bits.

TABLE II
SYSTEM PERFORMANCES (NOTE: * OBTAINED BY EXIT CHART)

p	Two Phases (dB)		Proposed Single Phase (dB)			
	η_{SW}	γ_{lim}	η_{SW}	γ_{lim}	γ_{BER}	Gap
0.00	0.2500	-7.2306	0.5000	-6.8381	-5.010	1.83
0.01	0.2702	-6.8619	0.5404	-6.4361	-4.135	2.30*
0.10	0.3673	-5.3776	0.7345	-4.7898	-2.135	2.59
0.20	0.4305	-4.5882	0.8609	-3.8922	-1.135	2.76*
0.30	0.4703	-4.1406	0.9406	-3.3753	-0.510	2.86*
0.40	0.4928	-3.9027	0.9855	-3.0980	-0.135	2.96*
0.49	0.4999	-3.8285	0.9999	-3.0112	0.000	3.01

1) Two-Phase Transmission: The capacity of a channel with two-phase transmission is given by

$$\mathcal{H}(b_1, b_2) \leq \mathcal{R}_1 + \mathcal{R}_2,$$
$$\leq \mathcal{C}_1/R_{c_1} + \mathcal{C}_2/R_{c_2},$$
$$\leq \frac{1}{R_c} \{\log_2(1 + \gamma_1) + \log_2(1 + \gamma_2)\}, \quad (17)$$

where $\mathcal{C}_1$ and $\mathcal{C}_2$ is the channel capacity for link between the singe receive antenna and transmit antenna 1 and 2, respectively. By assuming that $\gamma_1 = \gamma_2 = \gamma$ and $R_{c_1} = R_{c_2} = R_c = 1/2$, the SW/Shannon limit γ_{lim} and spectrum efficiency

$$\eta_{SW} = \frac{1}{2} R_c \mathcal{H}(b_1, b_2) \quad (18)$$

are shown in Table II.

2) Single Phase Transmission: With single phase transmission using single receive antenna, the capacity of SW is determined by the phase θ, where the MAC rate region for $P_1 = P_2 = P$, as shown in the Appendix, is given by

$$\mathcal{H}(b_1, b_2) \leq \frac{1}{R_c} \log_2 \left\{ \left(1 + \frac{P}{N}\right) \left(1 + \frac{P}{N + P \cos^2 \theta}\right) \right\}. \quad (19)$$

The total MAC capacity in (19) is maximum with $\theta = 90°$ regardless of P_1 and P_2 values, resulting in the same equation as the MAC capacity of two-phase transmission given by (17). On the contrary, the total capacity in (19) is minimum with $\theta = 0°$ which is equivalent to a capacity of multiple-input single output (MISO) channel,

$$\mathcal{H}(b_1, b_2) \leq \frac{1}{R_c} \log_2 \left\{ \left(1 + \frac{P}{N}\right) \left(1 + \frac{P}{N + P}\right) \right\}$$
$$\leq \frac{1}{R_c} \log_2(1 + 2\gamma). \quad (20)$$

The γ_{lim} for $\theta = 0°$ and its SW spectrum efficiency

$$\eta_{SW} = R_c \mathcal{H}(b_1, b_2) \quad (21)$$

for Fading MAC are also summarized in Table II.

B. Bit-Error-Rate (BER) Performances

BER performance is evaluated over Fading MAC with phase difference of $\theta = 0°$ and $\theta = random$. The results are plotted in Fig. 5 for $p = 0$, $p = 0.1$, and $p = 0.5$ (without correlation exploitation); for other p values, the results, in terms of SNR at BER $= 10^{-5}$, denoted as γ_{BER}, are estimated using EXIT
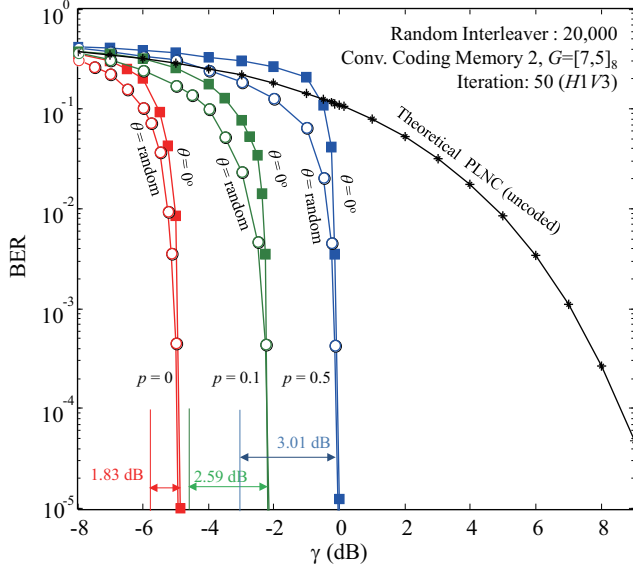
Fig. 5. BER performances of two correlated sources with correlation $p = \{0, 0.1\}$ and phase difference $\theta = \{0°, \text{random}\}$

chart; the results are presented in Table II. BER curve with uncoded physical layer network coding (PLNC)[13], expressed as [8], [15]

$$P_b = \frac{1}{2}\text{erfc}\left(\frac{T}{\sqrt{N}}\right) + \frac{1}{4}\text{erf}\left(\frac{T+2}{\sqrt{N}}\right) + \frac{1}{4}\text{erf}\left(\frac{T-2}{\sqrt{N}}\right), \quad (22)$$

are shown for a baseline comparison, where T is the optimum threshhold given by $T = 1 + \frac{N}{4}\ln(1 + \sqrt{1 - e^{-\frac{8}{N}}})$ [8], and $\text{erf}(x) = 1 - \text{erfc}(x)$.

It can be observed from Fig. 5 that the proposed SW-ISM for $p = 0$ provides clear turbo-cliff at $\gamma = -5.01$ dB, which is about 1.83 dB away from the SW/Shannon limit. It is also found that BER curves with $\theta = 0°$ and $\theta = random$ coincide at lower BER, which indicates that channel with $\theta = 0°$ dominates the performance. Therefore, we can approximate the BER for Fading MAC with instantaneous power control with single phase transmission, of which rate bound is given by (27) shown in Appendix, with $\theta = 0°$.[14] When the correlation $p = 0.1$, clear turbo-cliff is still achievable without error floor at $\gamma = 2.135$ dB, which is about 2.59 dB away from the limit.

The performances gap of the proposed SW-ISM for other p values increases as the correlation decreases as shown in Table II. A general tendency is that the smaller the correlation, the larger the distance to the SW/Shannon limit. For example, with $p = 0.5$, the threshold SNR is about 3.01 dB away from the limit.

C. Analysis on the Slepian-Wolf and Fading MAC Rate Regions

In this sub-section, we provide analysis of SW and MAC rate regions based on the results on Fading MAC channels

[13]It happens when the phase difference $\theta = 0°$.

[14]However, the ergodic capacity, as presented in the next subsection, is obviously larger.

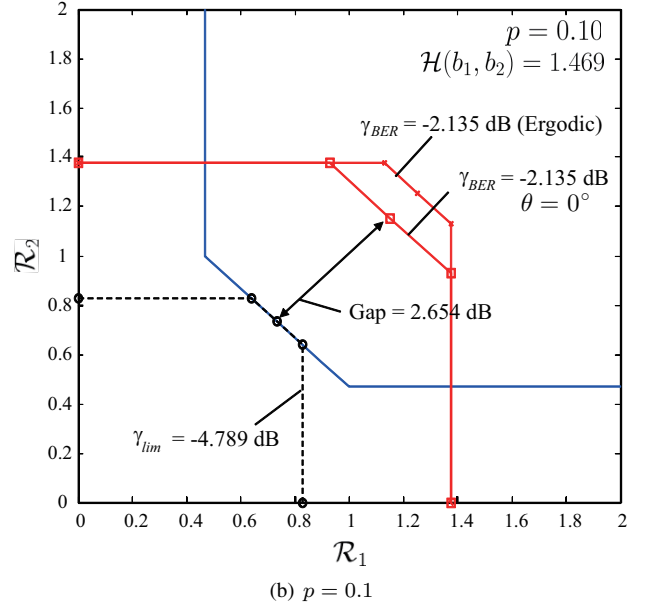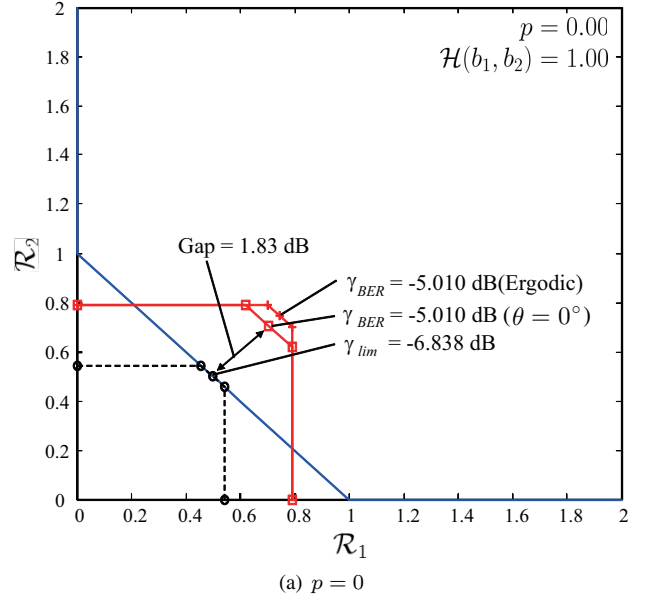

(a) $p = 0$

(b) $p = 0.1$

Fig. 6. Fading MAC (with instantaneous power control) and SW capacity rate regions

with instantaneous power control for $p = 0$ and $p = 0.1$. The results are shown in Fig. 6(a) and (b), respectively. The SW capacity rate region only depends on the correlation p and is independent of SNR. The theoretical MAC capacity rate region is shown with dashed line. The SW/Shannon theoretical SNR limit, defined for

$$\mathcal{H}(b_1, b_2) = \frac{1}{R_c}(\mathcal{C}_1 + \mathcal{C}_2) \quad (23)$$

is satisfied, which are at $\gamma_{lim} = -6.838$ dB and -2.135 dB for $p = 0$ and $p = 0.1$, respectively.

The MAC region evaluated at BER$= 10^{-5}$ by the proposed SW-ISM structure for $p = 0$ is shown in Fig. 6(a) with $\gamma_{BER} = -5.01$ dB. The gap from the theoretical limit is
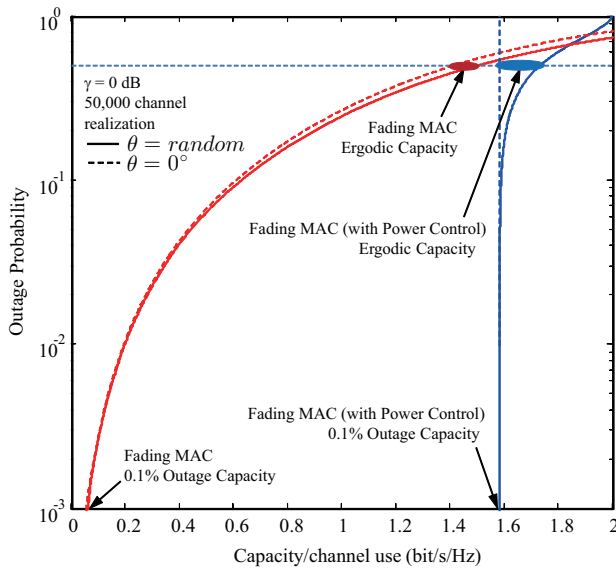
Fig. 7. Numerical evaluation of ergodic and outage capacities of Fading MAC with and without instantaneous power control at $\theta = 0°$ and $\theta = random$

1.83 dB as shown by the figure. The ergodic capacity with the same γ_{BER} is also shown in the figure. Fig. 6(b) shows the rate regions for $p = 0.1$, where the γ_{lim} is -2.135 dB. The gap from the theoretical limit is 2.654 dB, which is larger compared to the case of $p = 0$ as presented in Fig. 6(a) because of its weaker correlation.

The ergodic MAC capacity is obtained by numerical integration of (27), as shown in Appendix, over all θ values with uniform distribution $p(\theta) = \frac{1}{2\pi}$. However, as shown by Fig. 7, for $\gamma = 0$ dB, the capacity of $\theta = 0°$ and $\theta = random$ for Fading MAC with and without instantaneous power control coincide at outage probability less than 1%.

Since the BER performance was evaluated using massive simulations where more than 50,000 blocks were transmitted, the result was with the outage probability of 0.002%. It can be concluded from the results and analysis that with our proposed SW-ISM structure the SW and Fading MAC with instantaneous power control overlaps with 99.998% probability. Hence, the *source channel separation holds with the probability*.

VI. CONCLUSIONS

In this paper, we have proposed a simple coding structure for single carrier signalling of two correlated sources with *single phase* transmission where the receiver has only a single receive antenna and a very simple decoder. To achieve flexible adaptability to the correlation parameters, doped-accumulator is utilized. It has been found that a close matching between EXIT curves of demapper and decoder can be achieved, yielding the gap to the Slepian-Wolf/Shannon theoretical limit is about $1.83 - 3.01$ dB. In this paper, the rates of the two users were assumed to be the same. However, with a minor modifications, it can be easily proven that the same results can be derived in the asymmetric cases, including the well-

known corner points in the rate region corresponding to the successive cancellation. *The proposed structure has potential applications to cooperative relaying systems* that allow errors between the source and relay links with small number of transmission phases.

APPENDIX

In Fading MAC with instantaneous power control, we have $|h_1|^2 = |h_2|^2 = 1$ and $\angle(h_1, h_2) = \theta = random$. Since θ is a random variable, the achievable rates in Fading MAC are also random variables. By assuming that θ is known to the receiver and the noise N is complex Gaussian distributed, the rates can be expressed as

$$\mathcal{R}_1(\theta) \leq \log_2\left(1 + \frac{P}{N + P\cos^2\theta}\right), \quad (24)$$

$$\mathcal{R}_2(\theta) \leq \log_2\left(1 + \frac{P}{N + P\cos^2\theta}\right), \quad (25)$$

$$\mathcal{R}_1(\theta) + \mathcal{R}_2(\theta) \leq \log_2\left\{\left(1 + \frac{P}{N}\right)\left(1 + \frac{P}{N + P\cos^2\theta}\right)\right\}. \quad (26)$$

Finally, the average rate of Fading MAC, averaged over all the possible θ distributed by $p(\theta)$ over $(0, 2\pi]$, can be calculated from

$$\mathcal{R}_i \leq \int_0^{2\pi} \mathcal{R}_i(\theta)p(\theta)d\theta. \quad (27)$$

REFERENCES

[1] J. Chou, D. Petrovic, and K. Ramchandran, "A distributed and adaptive signal processing approach to reducing energy consumption in sensor networks," in *IEEE INFOCOM*, Sept. 2004.

[2] D. Slepian and J. K. Wolf, "Noiseless coding of correlated information sources," *IEEE Trans. on Info. Theory*, vol. 19, pp. 471–480, July 1973.

[3] Z. Xiong, A. D. Liveris, and S. Cheng, "Distributed source coding for sensor networks," *IEEE Signal Proc. Mag.*, pp. 80–94, Sept. 2004.

[4] R. Cristescu, B. Beferull-Lozano, and M. Vetterli, "Networked Slepian-Wolf: Theory, algorithm and scaling laws," *IEEE Trans. on Information Theory*, vol. 51, no. 12, pp. 4057–4073, Dec. 2005.

[5] F. Simoens, H. Wymeersch, and M. Moeneclaey, "Spatial mapping for MIMO systems," in *IEEE Inform. Theory Workshop*, 2004, pp. 187–192.

[6] J. Karjalainen, N. Veselinovic, K. Kansanen, and T. Matsumoto, "Iterative frequency domain joint-over-antenna detection in multiuser MIMO," *IEEE Trans. Wireless Comm.*, vol. 6, no. 10, pp. 3620–3631, 2007.

[7] S. ten Brink, "Convergence behavior of iteratively decoded parallel concatenated codes," *IEEE Trans. Commun.*, vol. 49, pp. 1727–1737, Oct. 2001.

[8] S. Zhang, S. C. Liew, and P. P. Lam, "Hot topic: Physical-layer network coding," in *ACM Mobicom*, California, Sept. 2006, pp. 358–365.

[9] K. Anwar and T. Matsumoto, "MIMO spatial turbo coding with iterative equalization," in *ITG Wireless Smart Antenna*, Feb. 2010.

[10] ——, "Spatially concatenated codes with turbo equalization for correlated sources," *Submitted to IEEE Trans. on Signal Processing*, 2011.

[11] T. M. Cover and J. A. Thomas, *Elements of Information Theory*, 2nd ed. Wiley-Interscience, 2006.

[12] K. Anwar and T. Matsumoto, "Very simple BICM-ID using repetition code and extended mapping with doped accumulator," *Springer Journal on Wireless Pers. Comm. (Online 13 Sept., DOI:10.1007/s11277-011-0397-1)*, 2011.

[13] J. Garcia-Frias and Y. Zhao, "Near-Shannon/Slepian-wolf performance for unknown correlated sources over AWGN channels," *IEEE Trans. on Comm.*, vol. 53, no. 4, pp. 555–559, April 2005.

[14] L. Bahl, J. Cocke, F. Jelinek, and J. Raviv, "Optimal decoding of linear codes for minimizing symbol error rate," *IEEE Trans. on Info. Theory*, vol. IT-20(2), pp. 284–287, March 1974.

[15] S. N. Islam and P. Sadeghi, "Error propagation in a multi-way relay channel," in *IEEE International Conference on Signal Processing and Communication System (ICSPCS)*, Honolulu, Dec. 2011, pp. 1–8.